Microchimica Acta
https://doi.org/10.1007/s00604-018-2719-4

ORIGINAL PAPER

A graphene modified carbon ionic liquid electrode for voltammetric analysis of the sequence of the *Staphylococcus aureus* nuc gene

Xueliang Niu[1] · Wei Chen[1,2] · Xiuli Wang[2] · Yongling Men[1] · Qin Wang[1] · Wei Sun[1,3] · Guangjiu Li[2]

Received: 19 January 2018 / Accepted: 28 January 2018
© Springer-Verlag GmbH Austria, part of Springer Nature 2018

Abstract

The authors describe a voltammetric method for the detection of the nuc ssDNA sequence originating from *Staphylococcus aureus* by using a carbon ionic liquid electrode modified with electrodeposited three-dimensional graphene (3DGR). Probe ssDNA was electrostatically adsorbed on the modified electrode by a potentiostatic method. The porous structure and large surface area of 3DGR greatly increase the amount of immobilized probe ssDNA on the interface, which is beneficial for the reaction with target ssDNA. By using Methylene Blue (MB) as the electrochemical probe, the reduction peak current of MB (best measured at −0.30 V vs. SCE) can be used for detecting hybridization. The differential pulse voltammetric current of MB increases linearly in the 1.0×10^{-12} mol L^{-1} to 1.0×10^{-6} mol L^{-1} nuc concentration range, and the detection limit is 3.3×10^{-13} mol L^{-1} (at 3σ). The DNA sensor was successfully applied to the determination of the PCR product of the gene in pork.

Keywords Electrochemical DNA biosensor · Three-dimensional graphene · Electrostatic adsorption · Potentiostatic reduction · Differential pulse voltammetry

Introduction

Electrochemical DNA biosensor is an efficient tool to analyze specific DNA sequences [1]. Due to the specific recognition process of DNA hybridization and the use of electroanalytical methods, electrochemical DNA biosensor has showed the properties including good sensitivity, less response time and cheap cost operation [2]. Nanomaterials such as metal and carbon with various morphologies have been applied to the preparation of electrochemical DNA sensing platform [3, 4]. Li et al. reported a functionalized multi-wall carbon nanotubes based electrochemical DNA sensor for breast cancer marker detection with the advantages sucn as time-consuming and low detection limit [5]. Gao et al. proposed an nanostructured electrochemical DNA biosensor for cauliflower mosaic virus with silver nanoparticles deposited on graphene oxide (GO) nanosheets modified gold electrode [6]. Chen et al. described a sandwich-type DNA sensor for *Mycobacterium tuberculosis* with polyaniline-reduced graphene as redox nanoprobe [7].

Graphene (GR) is a sp^2 bonded carbon nanosheet that exhibits specific performance including large interface area and high conductivity, which can fast the electron transfer rate and has certain electro-catalytic activity [8]. Electrochemical sensors with the usage of GR had been summarized with the properties including wide electrochemical windows, good biocompatibility and so on [9, 10]. In general GR is not stable in the aqueous solution and easily agglomerates by *van der Waals* and π restacking, that restricts its real applications. Three-dimensional (3D) GR has aroused in the

Electronic supplementary material The online version of this article (https://doi.org/10.1007/s00604-018-2719-4) contains supplementary material, which is available to authorized users.

✉ Wei Sun
swyy26@hotmail.com

[1] Key Laboratory of Tropical Medicinal Plant Chemistry of Ministry of Education, College of Chemistry and Chemical Engineering, Hainan Normal University, Haikou 571158, People's Republic of China

[2] College of Chemistry and Molecular Engineering, Qingdao University of Science and Technology, Qingdao 266042, People's Republic of China

[3] Key Laboratory of Soft Chemistry and Functional Materials of Ministry of Education, College of Chemical Engineering, Nanjing University of Science and Technology, Nanjing 210094, People's Republic of China

Published online: 10 February 2018

electrode modification [11]. By controlling the reaction conditions, various methods have been described for the fabrication of 3DGR and its related composites [12]. Among them electrodeposition is of higher efficiency and lower-cost. The operation is also easy to be realized by electrochemical methods including voltammetric technique or potentiostatic procedure [13]. Sheng et al. explored the fabrication of 3DGR electrode by one-step electrochemical reduction of GO, which showed outstanding performance in supercapacitor [14]. Wang et al. synthesized a 3DGR supported Pt nanoparticles nanocomposite by electrochemical method for methanol electrooxidation [15]. Tian et al. described the formation of 3DGR based on a two-step electrochemical synthesis, which showed promising application for bone tissue engineering [16].

Ionic liquid (IL) has unique performances including good chemical stability, fast ionic conductivity and stable electrochemical windows, which has been acted as supporting electrolyte or modifier of the working electrodes in electroanalysis [17]. Opallo et al. reported the electrochemical sensing of ILs [18]. When IL was used as the binder and/or the modifier in carbon paste electrode (CPE), carbon ionic liquid electrode (CILE) was constructed with high conductivity and remarkable electrocatalytic activity [19]. The high viscosity of IL can bind the graphite powder together with good dispersion. Also a layer of IL can be formed on the surface of graphite powder, which provides the organic groups for the further reaction. Momeni et al. used a nanostructured copper hydroxide modified CILE to voltammetric detection of metformin [20]. We have fabricated CILE or modified CILE as the substrate electrodes to construct electrochemical sensing devices [21–23]. The combinations of modifiers with CILE often provide an excellent electrochemical platform for the sensing applications.

In this paper 1-hetylpyridinium hexafluorophosphate ($HPPF_6$) was selected to fabricate CILE due to its good electrochemical performance [24]. On CILE surface 3DGR was decorated by electrodeposition to get 3DGR/CILE. Then the probe oligonucleotide sequence was immobilized on 3DGR/CILE by electrostatic adsorption to obtain a DNA modified electrode. The presence of large surface 3DGR with interconnect porous structure increases the surface concentration of oligonucleotide sequence and its high conductivity is good for electron transfer. Methylene blue (MB) is chosen as the electrochemical indicator due to its excellent distinguish ability to ssDNA and dsDNA, and the responses of MB were enhanced greatly with the sensitivity for target ssDNA sequence detection increased. This new DNA sensing method was further used for the nuc sequences from *Staphylococcus aureus* and its polymerase chain reaction (PCR) product analysis successfully.

Experimental

Apparatus and reagents

Electrochemical experiments were performed with CHI 750B electrochemical analyzer (Shanghai CH Instrument, China, http://www.chinstr.com). Three-electrode procedure was used with saturated calomel reference electrode (SCE), platinum wire counter electrode and 3DGR/CILE working electrode ($\Phi = 4$ mm). Photos of scanning electron microscopy (SEM) and energy dispersive x-ray spectroscopy (EDS) were recorded on JSM-7100F field emission scanning electron microscope (Japan Electron Company, Japan, https://www.jeol.co.jp) equipped with x-ray energy dispersive spectrometer (INCA X-act, Oxford Instruments, United Kingdom, http://www.oxford-instruments.cn) with the operating voltage of 5.0 kV and 20 kV, respectively.

$HPPF_6$ (>99%, Lanzhou Yulu Fine Chemical Ltd. Co., China, http://www.ilssale.com), GO (>98.5%, average size of 0.4–1.0 μm, average layer thickness of 0.73 nm and C/O ratio of 1.4, Garmery Materials Technology Co., China, http://www.sinocarbon-cas.com), graphite powder with average size of 30 μm (Shanghai Colloid Chemical Ltd. Co., China, https://shjthg.cn.china.cn), MB (AR grade, Tianjin Yongda Chemical Reagent Ltd. Co., China, http://www.tjydhxsj.com) and $LiClO_4$ (>99%, Chengdu Kelong Chemical Ltd. Co., China, http://www.chronchem.com/cn) are purchased commercially. Other reagents are of analytical reagent grade with doubly distilled water for aqueous solution.

The 22-Base ssDNA nuc gene sequences are from *Staphylococcus aureus* O46 chromosome, complete genome sequence ID: CP025395.1, which are provided by Shanghai Sangon Biological Ltd. Co. (China, http://www.sangon.com), and used according to the instruction without further purification. The sequences are as follows:

probe ssDNA: 5′-TGG ACG TGG CTT AGC GTA TAT T-3′;
target ssDNA: 5′-AAT ATA CGC TAA GCC ACG TCC A-3′;
one-base mismatched ssDNA: 5′- AAG ATA CGC TAA GCC ACG TCC A-3′;
three-base mismatched ssDNA: 5′- AAG ATA CGC TAC GCC ACG TCT A-3′;
non-complementary ssDNA: 5′-GCG GTT GAA TCG GCG ATG GGT G-3′.

PCR experiment was realized with Eppendorf Mastercycler Gradient PCR system (Eppendorf, Germany) and oligonucleotide primers used are as follows:

Primer F: 5′-CCT GAA GCA AGT GCA TTT ACG A-3′;
Primer R: 5′-CTT TAG CCA AGC CTT GAC GAA CT-3′.

Electrode fabrication

CILE was prepared as substrate solid electrode using the former procedure [11] and polished before use. Then 3DGR decorated electrode was fabricated with potentiostatic method that reported previously with little modifications [14]. By putting CILE into a mixture solution of 3.0 mg mL^{-1} GO and 0.1 mol L^{-1} $LiClO_4$, potentiostatic reduction was performed at a fixed potential (−1.30 V) for 300 s with magnetic stirring. After that CILE was took out, rinsed with water and dried by N_2 gas to get 3DGR/CILE.

Construction of electrochemical DNA sensor

The prepared 3DGR/CILE was immersed in a 1.0×10^{-6} mol L^{-1} probe ssDNA sequence with 50.0 mmol L^{-1} pH 7.0 PBS. After fixing the potential at +0.5 V for 400 s, probe ssDNA sequence was modified on 3DGR/CILE by electrostatic adsorption, which was named as ssDNA/3DGR/CILE. Then it was cleaned by 0.5% sodium dodecyl sulfate (SDS) solution and water three-times in turn.

Hybridization was carried out with dropping 10.0 μL target ssDNA sequence solution (in 50.0 mmol L^{-1} PBS) on ssDNA/3DGR/CILE and reacted for 30 min at 25 °C. After that the electrode was further cleaned by 0.5% SDS solution and water for three-times to get dsDNA/3DGR/CILE.

Voltammetric analysis

The dsDNA/3DGR/CILE was used as the working electrode, which was inserted inside 2.0×10^{-5} mol L^{-1} MB (in 50.0 mmol L^{-1} pH 7.0 Tris-HCl) solution for 10 min accumulation with the following washing with 50.0 mmol/L PBS (3 times). Then three-electrode system was put into a 50.0 mmol L^{-1} pH 7.0 Tris-HCl buffer and differential pulse voltammetric curves were scanned in the electrochemical window from 0.2 V to −0.7 V. The instrumental parameters were: pulse amplitude 0.05 V, pulse width 0.05 s and pulse period 0.2 s. All the voltammetric data is the average value of three times parallel measurements ($n = 3$). Scheme 1 displays the fabrication and detection procedure of this obtained electrochemical DNA biosensor.

Procedure of PCR

The spoiled pork was used as samples, which was mixed with 10 mL *Staphylococcus aureus* enrichment broth base (BJ-PYJ0285, Jingbang, Shanghai, China) and incubated in 25 °C water bath for 2 days. Then the sample solution was centrifuged at 12000 rpm for 240 s to obtain the precipitate, which was re-dispersed by 100 μL sterilized water and used for DNA extraction with DNA extraction kit (Beijing Tiangen Biotech. Ltd. Co., China).

PCR amplification of nuc sequence was performed in a 25 μL solution, which was composed of 200.0 nmol L^{-1} primer F and primer R, 10 × reaction buffer B, 2.0 mmol L^{-1} $MgCl_2$, 200.0 nmol L^{-1} of dATP, dCTP, dGTP and dTTP, 1.5 units of Taq DNA polymerase, and 1.0 μL template from samples. The experiment was performed by initially denaturation of DNA at 94 °C (30 s), and then set for 35 cycles of amplification (94 °C, 30 s; 56 °C, 30 s; 72 °C, 30 s) with final extension at 72 °C (300 s).

Results and discussion

Choice of materials

3DGR has the merits of connected conductive networks, fast mass transfer rate and large specific surface area, which can be synthesized by electrodeposition directly on CILE electrode surface. Also CILE has the advantages such as high conductivity, wide potential window, outstanding anti-fouling ability and stability. Therefore the combination of 3DGR with CILE can result in a specific biosensing interface for the DNA immobilization with increased sensitivity.

Characteristics of electrodes

Figure 1a shows SEM image of 3DGR/CILE, indicating an interconnected and porous microstructure of 3DGR, which is in good consistence with the previous paper using similar procedure [7]. The elemental EDS mapping image of 3DGR on CILE surface is shown in Fig. 1b, which give the uniform distribution of C and O elements. And the atomic ratio of 5.3:1 is calculated by elemental analysis, which is much higher than that of GO (1.4:1), implying the reduction of GO with the reducing of O-containing groups [25]. Electrochemical reduction is an effective and controllable method to synthesize 3DGR. The 3D structure on the electrode can provide an increased interface area that is favorable for the further fixation of ssDNA sequence. Therefore ssDNA sequence was loaded on 3DGR/CILE due to the attraction by carbon materials at selected potential.

Raman spectroscopy is an effective technique to monitor GR layers, defects and strain and so on [26]. As for GO in Fig. 1c, two obvious peaks at approximately 1339 cm^{-1} and 1596 cm^{-1} are observed, which are typically corresponding to D and G bands [27]. The D band is associated with A_{1g} mode and reflects the defects and edges in graphite material. The G band is aroused from the E_{2g} mode, originating from the in-plane sp^2 C=C stretching motion [28]. The intensity ratio of D and G bands (I_D/I_G) for 3DGR is estimated as 1.27, which is larger than that of GO precursor (1.06), revealing that the sp^2 domains decreased upon the formation of 3DGR [29]. The results can be due to the increasing

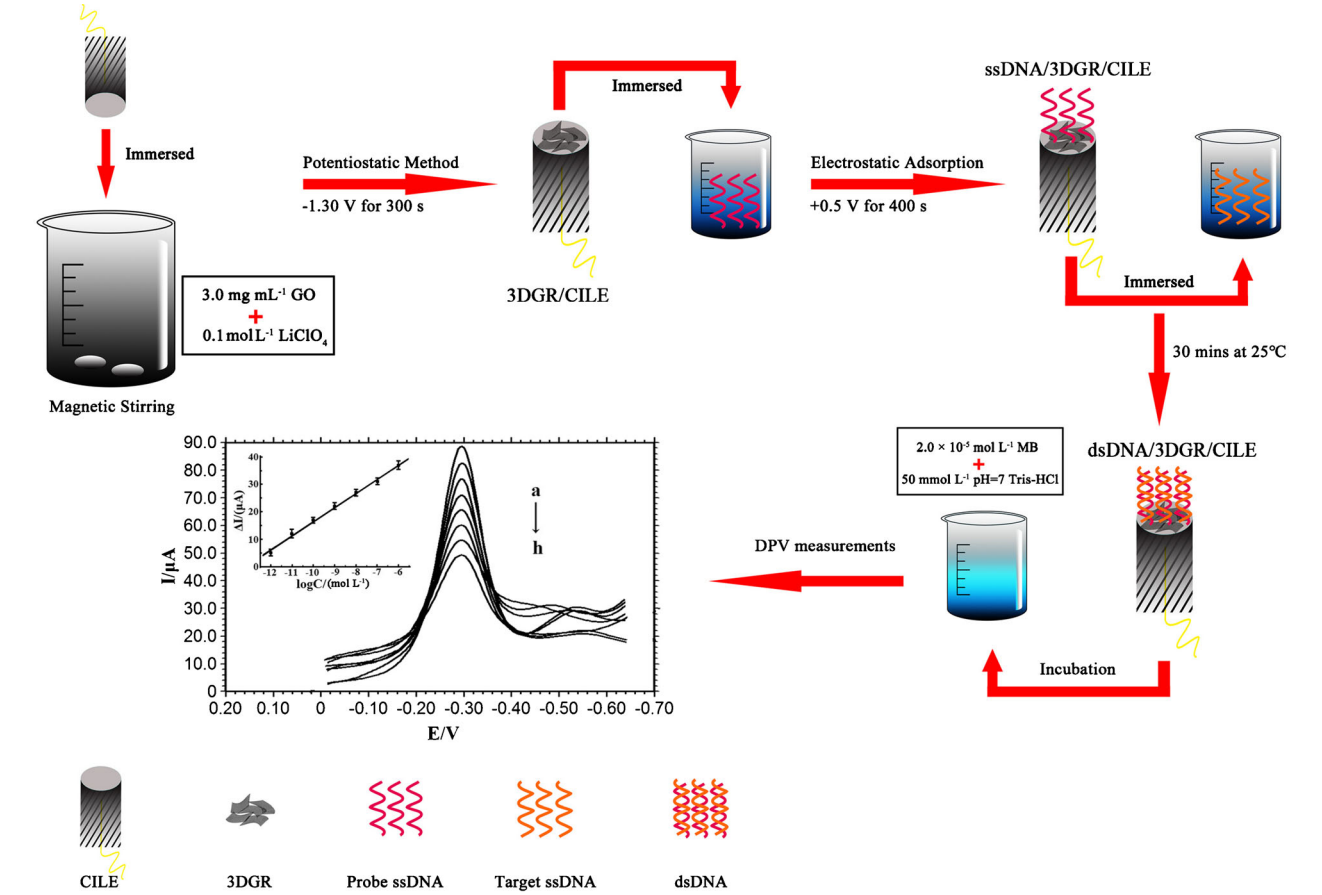

Scheme 1 Fabrication and detection process of this electrochemical DNA biosensor

trend in the formation of new domains of conjugated C atoms and the increasing defect density, which is indicative of the partially reduction of GO during the electrodeposition process [16]. In addition, well-defined peaks of 2D band at 2678 cm^{-1} and (D + G) band at 2916 cm^{-1} are obviously observed, also indicating the efficient reduction of GO by electrochemical technique [30].

Cyclic voltammograms of four electrodes were scanned with curves overlapped in Fig. 2a. Well-defined redox peaks of ferricyanide are observed with different responses. On 3DGR/CILE (curve d) the responses are larger than that of CILE (curve a) with the background current increased, indicating that the high conductive 3DGR with porous structure can increase the Faraday's current and charging current. The specific π interaction between aromatic groups of IL molecule with the π-electronic GR is also existed on the electrode with the stability increased [31]. The presence of probe ssDNA sequence on 3DGR/CILE leads to the decrease of redox peak currents of ferricyanide (curve c) and the current responses on dsDNA/3DGR/CILE (curve b) are further decreased. The

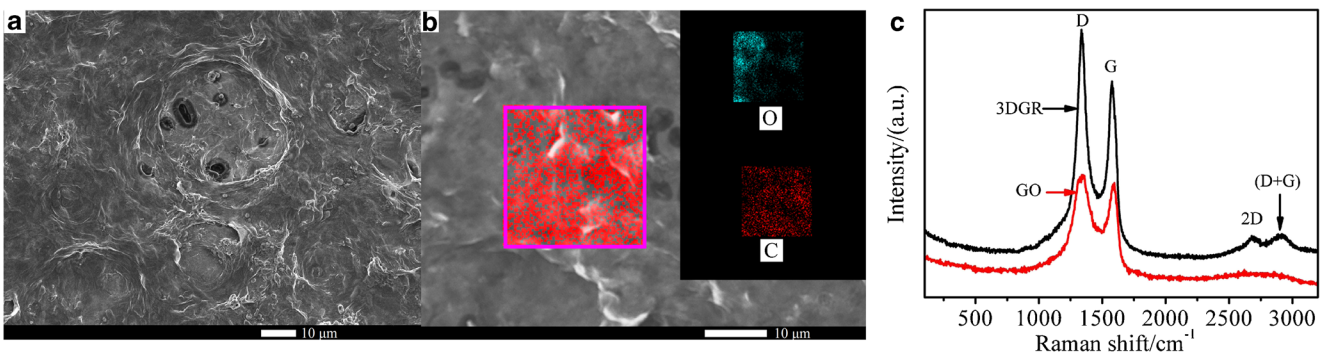

Fig. 1 **a** SEM image of the surface of 3DGR/CILE; **b** The EDS mapping image of 3DGR on CILE; (C) Raman spectra of 3DGR compared with GO

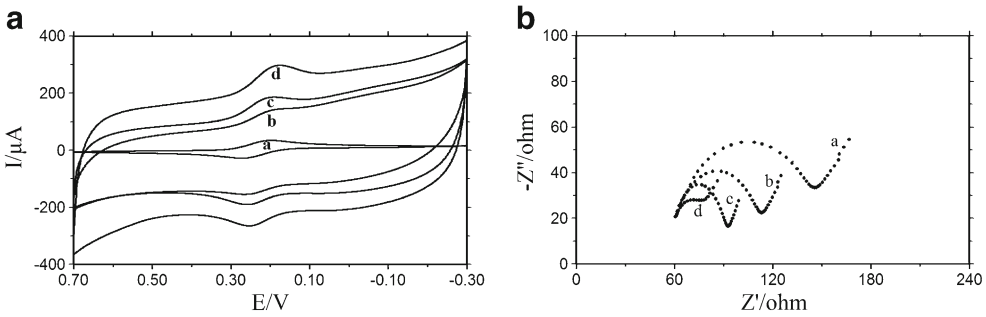

Fig. 2 **a** Cyclic voltammograms of different electrodes in 1.0 mmol L^{-1} $K_3[Fe(CN)_6]$ and 0.5 mol L^{-1} KCl solution; **b** EIS of different electrodes in 10.0 mmol L^{-1} $[Fe(CN)_6]^{3-/4-}$ and 0.1 mol L^{-1} KCl solution. Electrodes used from a to d were CILE, dsDNA/3DGR/CILE, ssDNA/3DGR/CILE and 3DGR/CILE

phenomenon can be ascribed to the negatively charged DNA molecules on the electrode surface blocked the electron transfer of $[Fe(CN)_6]^{3-/4-}$ from the solution. The electroactive surface area (A) of electrodes were calculated according to Randles–Sevcik eq. [32] with $[Fe(CN)_6]^{3-/4-}$ (1.0 mmol L^{-1}) as electrolyte. The plot of I_{pc} against the square of scan rate ($\upsilon^{1/2}$) was shown in Fig. S1, from which 0.365 cm^2 was estimated for 3DGR/CILE. The result is 1.8 times larger than that of CILE (0.204 cm^2), indicating that the presence of 3DGR can provide larger platform for ssDNA modification.

Electrochemical impedance spectroscopy (EIS) can record the interfacial impedance changes after modification, which was performed in a 10.0 mmol L^{-1} $[Fe(CN)_6]^{3-/4-}$ and 0.1 mol L^{-1} KCl mixture solution with curves listed in Fig. 2b. The resistance of electron transfer (R_{et}) of CILE (curve a) was 145.71 Ω with that of 3DGR/CILE (curve d) as 75.30 Ω, indicating the high conductive 3DGR on the electrode lowered the interfacial resistance. On ssDNA/3DGR/CILE (curve c) and dsDNA/3DGR/CILE (curve b), the R_{et} value increased to 111.43 Ω and 150.2 Ω, proving the electrostatic repulsion was present among the polyanion in DNA structure and the negatively charged $[Fe(CN)_6]^{3-/4-}$. These data indicated that DNA was successful immobilized on 3DGR/CILE by electrostatic adsorption. Electroadsorption is a commonly used method for DNA immobilization on carbon material, which has been reported in the preparation of electrochemical DNA sensor [33]. At 3DGR modified electrode ssDNA is adsorbed at the positive potential by electrostatic effects and the porous structure of 3DGR increases the adsorption amounts, therefore the ssDNA modified electrode can exhibit better performance.

Electrochemical investigation of the modified electrodes

MB is often selected as an electrochemical indicator in DNA sensing with excellent distinguish ability to dsDNA or ssDNA sequence [34]. It has been reported that MB has three interaction models with DNA, including electrostatic binding, grooves intercalation and preferential binding of MB with guanine bases [35]. As shown in Fig. 3, DPV curves of MB on various electrodes were recorded with a reduction peak located at −0.30 V (vs. SCE), a typical reductive reaction of phenothiazine group of MB [36]. On ssDNA/3DGR/CILE (curve d) the largest responses indicated the synergistic effects of ssDNA and 3DGR on electrode. The increase of effective area of 3DGR can enrich the loading of ssDNA with more guanines present for the accumulation of MB molecules. The high conductivity of 3DGR can also fast the electron transfer of MB molecules. Therefore the largest current value appeared on ssDNA and 3DGR co-modified CILE.

Optimization of the experimental conditions

The conditions including MB concentration and adsorption time of probe ssDNA were optimized with the results as 2.0×10^{-5} mol L^{-1} and 8 min respectively. Detailed data and figures are shown in the ESI and Fig. S1.

Selectivity

Selectivity was checked by the hybridization using the electrochemical DNA sensor with various mismatched ssDNA sequences and the results were summarized in Fig. 4. On ssDNA/3DGR/CILE (curve a) the largest peak current is ascribed to the electrode reaction of MB that interacted with

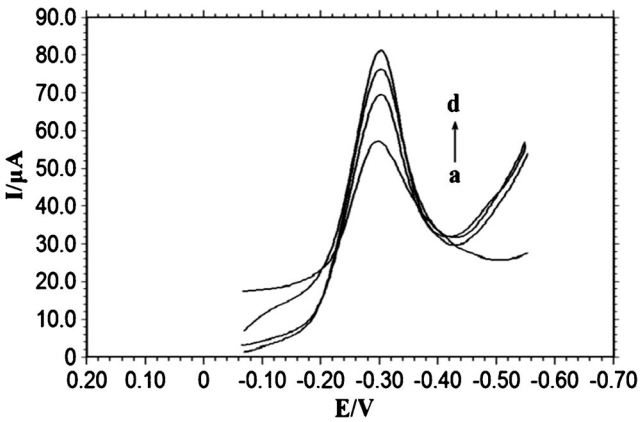

Fig. 3 Differential pulse voltammograms of 2.0×10^{-5} mol/L MB on (a) CILE, (b) ssDNA/CILE, (c) 3DGR/CILE and (d) ssDNA/3DGR/CILE

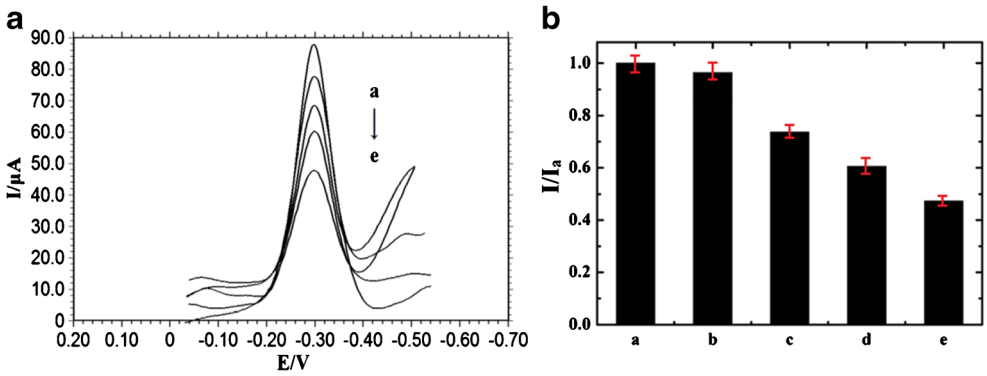

Fig. 4 **a** Differential pulse voltammograms and (**b**) histograms of 2.0×10^{-5} mol/L MB on ssDNA/3DGR/CILE (a) and after hybridization with the noncomplementary sequence (b), three-base mismatched sequence (c), one-base mismatched sequence (d) and complementary sequence (e)

guanine bases on probe ssDNA sequence. Hybridization with complementary ssDNA sequence results in the smallest peak current (curve e, 47.4% of the initial response), which is due to the formation of dsDNA on the electrode surface that prevented the interaction of MB and guanine on ssDNA. Hybridization with noncomplementary ssDNA sequence has 96.8% of the initial value (curve b), indicating that no hybridization take place on the electrode surface. The nonspecific adsorption of noncomplementary ssDNA sequence is present and can block the interaction of MB with guanine. Hybridization with three-base (curve c) and one-base (curve d) mismatched sequence result in 73.7% and 60.5% of the initial value, showing that the mismatched ssDNA can hybrid with the probe ssDNA on the electrode surface with the partially formation of dsDNA, which limits the amount of guanine residues to interact with MB. The result proves that high selectivity with excellent distinguish ability is achieved for analysis of various ssDNA sequences.

Sensitivity and stability

Target ssDNA sequences were detected by this method with curves overlapped in Fig. 5. Hybridization resulted in the decrease of the current of MB along with the increase of target ssDNA concentration, indicating that probe ssDNA sequence took part in hybridization with dsDNA formed on the electrode surface gradually. Therefore the interaction of guanine bases on ssDNA sequence with MB was hindered and less MB molecules existed on the electrode with the reduction current of MB became smaller. When the concentration was smaller than 1.0×10^{-12} mol L^{-1}, the current of MB at −0.30 V (vs. SCE) was almost unchanged. The differences of the current value (ΔI_p) of MB before and after hybridization showed a good linear relationship with the logarithmic value of target ssDNA sequence concentration from 1.0×10^{-12} mol L^{-1} to 1.0×10^{-6} mol L^{-1}. The regression equation was plotted as $\Delta I_p(\mu A) = 5.14\log[C/(\text{mol L}^{-1})] + 67.9$ ($n = 7$, $\gamma = 0.998$) with the sensitivity calculated as 84.82 μA/(μmol L^{-1} cm^2). The detection limit (DL) was estimated as 3.33×10^{-13} mol L^{-1} (3σ), which was smaller than a previous report with electro-reduced GR modified CILE for the detection of MON810 (4.52×10^{-12} mol L^{-1}) [37], indicating that the surface area of 3DGR/CILE was larger than that of GR nanosheet modified CILE. Therefore more probe ssDNA sequence was present on the electrode surface for the further hybridization with improved sensitivity. Also a systematic comparison of the analytical parameters of electrochemical DNA sensors was summarized in Table 1, which indicated the method had good analytical performance. Seven ssDNA/3DGR/CILEs were prepared and used for the detection of 1.0×10^{-8} mol L^{-1} target ssDNA sequence with the relative standard deviation (RSD) got to be 3.65%, proving the good repeatability of the preparation procedure. In addition, after a week storage of ssDNA/3DGR/CILE, the ΔI_p value for 1.0×10^{-8} mol L^{-1} target ssDNA sequence is about 97.86% of its initial determination value. The results above indicate good stability of this DNA biosensor.

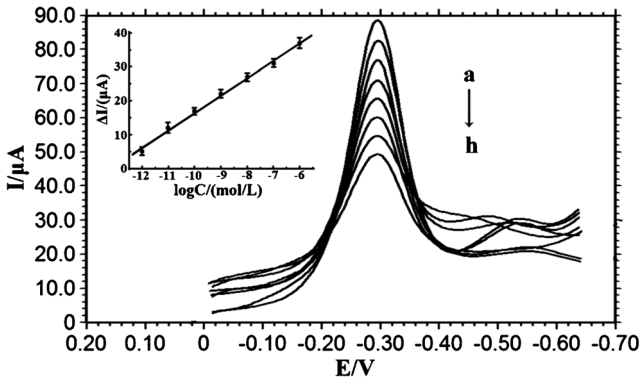

Fig. 5 Differential pulse voltammograms of MB on ssDNA/3DGR/CILE (a) and hybridization with target ssDNA sequence (from a to h were 0, 1.0×10^{-12}, 1.0×10^{-11}, 1.0×10^{-10}, 1.0×10^{-9}, 1.0×10^{-8}, 1.0×10^{-7} and 1.0×10^{-6} mol L^{-1}, respectively). Insert: plots of the ΔI_p versus log C

PCR product analysis

Sample of nuc gene from pork was amplified by PCR and further analyzed by electrochemical DNA sensor. The PCR

Table 1 Comparison of performances of different electrochemical DNA biosensors

Electrodes	Indicators	Methods	Linear range (mol L^{-1})	DL (mol L^{-1})	Ref.
ERG/CILE	MB	DPV	1.0×10^{-11}-1.0×10^{-6}	4.52×10^{-12}	[37]
CTS-Co_3O_4-GR/CILE	MB	DPV	1.0×10^{-12}-1.0×10^{-6}	4.3×10^{-13}	[38]
rGO/SPE	–	DPV	2.5×10^{-12}-7.5×10^{-11} 7.5×10^{-11}-7.5×10^{-9}	1.5×10^{-12}	[39]
MCH/SH-P1/AuNPs/PGE	–	DPV	2.0×10^{-10}-3.9×10^{-7}	1.0×10^{-10}	[40]
SPGE	–	EIS	2.0×10^{-11}-1.5×10^{-7}	8.5×10^{-12}	[41]
MWNTs-COOH/GCE	Daunomycin	DPV	2.0×10^{-10}-5.0×10^{-8}	1.0×10^{-10}	[42]
AuNPs/TB-GO/GCE	–	DPV	1.0×10^{-11}-1.0×10^{-9}	2.9×10^{-12}	[43]
ECR/GCE	MB	DPV	5.0×10^{-12}-2.0×10^{-10}	9.8×10^{-11}	[44]
Al(III)/CPE	MB	DPV	1.0×10^{-7}-1.0×10^{-4}	2.3×10^{-8}	[45]
aptamer/rGO-ssDNA-AuNPs/GCE	–	EIS	10–1.0×10^{6} cfu mL^{-1}	10 cfu mL^{-1}	[46]
3DGR/CILE	MB	DPV	1.0×10^{-12}-1.0×10^{-6}	3.3×10^{-13}	This study

ERG, electrochemical reduced graphene; *rGO*, reduced graphene oxide; *SPE*, screen-printed electrode; *MCH*, 6-mercapto-1-hexanol; *SH-P1*, thiol terminated capture probe 1; *AuNPs*, Au nanoparticles; *PGE*, pencil graphite electrode; *SPGE*, screen-printed gold electrode; *MWNTs-COOH*, multi-walled carbon nanotubes functionalized with a carboxylic acid group; *GCE*, glassy carbon electrode; *TB-GO*, toluidine blue-graphene oxide; *ECR*, eriochrome cyanine R

product solution was diluted with 50.0 mmol L^{-1} PBS, water-heated at 100 °C for 10 min and frozen in ice-bath for 2 min. The resulted ssDNA sample solution (10 μL) was dropped on the surface of ssDNA/3DGR/CILE with hybridization and voltammetric detection performed based on the procedure. As shown in Fig. 6, the reduction peak of MB on 3DGR/CILE (curve c) is estimated about 34.53 μA (RSD, 2.1%), which is smaller than 59.65 μA (RSD, 1.8%) on ssDNA/3DGR/CILE (curve a). The result is ascribed to the reaction of MB with guanine bases of ssDNA sequence present on the electrode with accumulation effect. Hybridization with the PCR sample results in the decrease of MB current to 39.77 μA (RSD, 2.7%, curve b), indicating the formation of dsDNA with less MB bound. Therefore the method can be used for the detection of sample solution containing the target ssDNA sequence.

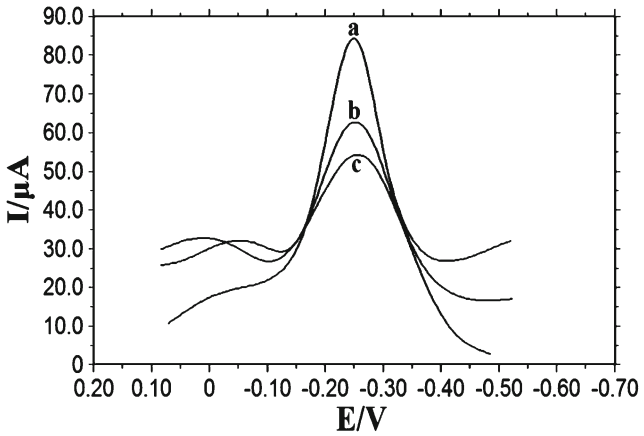

Fig. 6 Differential pulse voltammograms of MB on ssDNA/3DGR/CILE (a), after hybridized with PCR product of *Staphylococcus aureus* nuc sequence (b) and 3DGR/CILE (c)

Conclusions

By using the electrodeposited 3DGR modified electrode as the working electrode, an electrochemical DNA sensor is constructed by immobilization of probe ssDNA sequence on 3DGR/CILE with electrostatic adsorption. 3DGR has large surface area and porous structure, which can act as interface for increasing the adsorption amount of probe ssDNA sequence. Also the interfacial conductivity is accelerated on 3DGR modified electrode surface. Therefore the voltammetric current of MB on the modified electrode is enhanced greatly due to the synergistic functions of the modifiers. This electrochemical DNA sensor has the properties including low-cost process, good sensitivity and low detection limit, which exhibits the potential application in specific ssDNA sequences detection. The 3DGR modified electrode can also be applied in the fields of electrochemical sensors or biosensors with extensive usage. However, the electrostatic adsorption of ssDNA sequence on the electrode surface is random, which limits its hybridization effects due to the disorderly arrangement.

Acknowledgements The financial support by the National Natural Science Foundation of China (21665007), the Program for Innovative Research Team in University (IRT-16R19), the Natural Science Foundation of Hainan Province (2017CXTD007), the Key Science and Technology Program of Haikou City (2017042) and the Fundamental Research Funds for the Central Universities (30916014103) are gratefully acknowledged.

Compliance with ethical standards

The authors declare that they have no competing interests.

References

1. Pividori MI, Merkoç A, Alegret S (2000) Electrochemical genosensor design: immobilisation of oligonucleotides onto transducer surfaces and detection methods. Biosens Bioelectron 15:291–303
2. Mao X, Liu GD, Biomed J (2008) Nanomaterial based electrochemical DNA biosensors and bioassays. Nanotechnology 4:419–431
3. Rasheed PA, Sandhyarani N (2017) Electrochemical DNA sensors based on the use of gold nanoparticles: a review on recent developments Pathath Abdul Rasheed Neelakandapillai Sandhyarani. Microchim Acta 184:981–1000
4. Rasheed PA, Sandhyarani N (2017) Carbon nanostructures as immobilization platform for DNA: a review on current progress in electrochemical DNA sensors. Biosens Bioelectron 97:226–237
5. Li JF, Lee EC (2017) Functionalized multi-wall carbon nanotubes as an efficient additive for electrochemical DNA sensor. Sensors Actuators B 239:652–659
6. Gao NN, Gao F, He SY, Zhu QH, Huang JF, Tanaka H, Wang QX (2017) Graphene oxide directed in-situ deposition of electroactive silver nanoparticles and its electrochemical sensing application for DNA analysis. Anal Chim Acta 951:58–67
7. Chen YH, Li YL, Yang Y, Wu FN, Cao J, Bai LJ (2017) A polyaniline-reduced graphene oxide nanocomposite as a redox nanoprobe in a voltammetric DNA biosensor for mycobacterium tuberculosis. Microchim Acta 184:1801–1808
8. Bahadır EB, Sezgintürk MK (2016) Applications of graphene in electrochemical sensing and biosensing. Trac-Trend Anal Chem 76: 1–14
9. Xu JH, Wang YZ, Hu SS (2017) Nanocomposites of graphene and graphene oxides: synthesis, molecular functionalization and application in electrochemical sensors and biosensors. Microchim Acta 184:1–44
10. Song Y, Luo Y, Zhu C, Li H, Du D, Lin Y (2016) Recent advances in electrochemical biosensors based on graphene two-dimensional nanomaterials. Biosens Bioelectron 76:195–212
11. Sun W, Hou F, Gong SX, Han L, Wang WC, Shi F, Xi JW, Wang XL, Li GJ (2015) Direct electrochemistry and electrocatalysis of hemoglobin on three-dimensional graphene modified carbon ionic liquid electrode. Sensors Actuators B Chem 219:331–337
12. Yan Z, Yao W, Hu L, Liu D, Wang C, Lee CS (2015) Progress in preparation and application of three-dimensional graphene-based porous nano composites. Nano 7:5563–5577
13. Chen KW, Chen LB, Chen YQ, Bai H, Li L (2012) Three-dimensional porous graphene-based composite materials: electrochemical synthesis and application. J Mater Chem 22:20968
14. Sheng KX, Sun YQ, Li C, Yuan WJ, Shi GQ (2012) Ultrahigh-rate supercapacitors based on eletrochemically reduced graphene oxide for ac line-filtering. Sci Rep 2:247–253
15. Wang XF, Niu XL, Sha HL, Shi F, Chen W, Ma DX, Sun W (2016) Application of platinum nanoparticles decorated three-dimensional graphene modified electrode for methanol electrooxidation. Int J Electrochem Sci 11:7395–7400
16. Tian ZZ, Huang LX, Pei XB, Chen JY, Wang T, Yang T, Qin H, Sui L, Wang J (2017) Electrochemical synthesis of three-dimensional porous reduced graphene oxide film: preparation and in vitro osteogenic activity evaluation. Colloids Surface B 155:150–158
17. Shiddiky MJA, Torriero AAJ (2011) Application of ionic liquids in electrochemical sensing systems. Biosens Bioelectron 26:1775–1787
18. Opallo M, Lesniewski A (2011) A review on electrodes modified with ionic liquids. J Electroanal Chem 65:2–16
19. Maleki N, Safavi A, Farjami E, Tajabadi F (2008) Palladium nanoparticle decorated carbon ionic liquid electrode for highly efficient electrocatalytic oxidation and determination of hydrazine. Anal Chim Acta 611:151–155
20. Momeni S, Farrokhnia M, Karimi S, Nabipour I (2016) Copper hydroxide nanostructure-modified carbon ionic liquid electrode as an efficient voltammetric sensor for detection of metformin: a theoretical and experimental study. Iran J Chem Soc 13:1027–1035
21. Shi F, Zheng WZ, Wang WC, Hou F, Lei BX, Sun ZF, Sun W (2015) Application of graphene–copper sulfide nanocomposite modified electrode for electrochemistry and electrocatalysis of hemoglobin. Biosens Bioelectron 64:131–137
22. Niu XL, Zheng W, Yin CX, Weng WJ, Li GJ, Sun W, Men YL (2017) Electrochemical DNA biosensor based on gold nanoparticles and partially reduced graphene oxide modified electrode for the detection of listeria monocytogenes hly gene sequence. J Electroanal Chem 806:116–122
23. Chen W, Niu XL, Li XY, Li XB, Li GJ, He BL, Li QT, Sun W (2017) Investigation on direct electrochemical and electrocatalytic behavior of hemoglobin on palladium-graphene modified electrode. Mater Sci Eng C-Mater 80:135–140
24. Yan LJ, Wang XF, Li QT, Sun W (2016) Direct electrochemistry of horseradish peroxidase on NiO nanoflower modified electrode and its electrocatalytic activity. Croat Chem Acta 89:331–337
25. Ren PG, Yan DX, Ji X, Chen T, Li ZM (2011) Temperature dependence of graphene oxide reduced by hydrazine hydrate. Nanotechnology 22:055705
26. Chen ZP, Ren WC, Gao LB, Liu BL, Pei SF, Cheng HM (2011) Three-dimensional flexible and conductive interconnected graphene networks grown by chemical vapour deposition. Nat Mater 10:424–428
27. Malard LM, Pimenta MA, Dresselhaus G (2009) Dresselhaus MS, Raman spectroscopy in graphene. Phys Rep-Rev Sec Phys Lett 473:51–87
28. Liu HT, Zhang L, Guo YL, Cheng C, Yang LJ, Jiang L, Yu G, Hu WP, Liu YQ, Zhu DB (2013) Reduction of grapheme oxide to highly conductive graphene by Lawesson's reagent and its electrical applications. J Mater Chem C 1:3104–3109
29. Hou CY, Zhang QH, Li YG, Wang HZ (2012) Graphene-polymer hydrogels with stimulus-sensitive volume changes. Carbon 50: 1959–1965
30. Zhang QQ, Xu X, Li H, Xiong GP, Hu H, Fisher TS (2015) Mechanically robust honeycomb graphene aerogel multifunctional polymer composites. Carbon 93:659–670
31. Ruan CX, Li TT, Niu QJ, Lu M, Lou J, Gao WM, Sun W (2012) Electrochemical myoglobin biosensor based on graphene-ionic liquid-chitosan bionanocomposites: direct electrochemistry and electrocatalysis. Electrochim Acta 64:183–189
32. Bard AJ, Faulkner LR (2001) Electrochemical methods: fundamentals and applications, 2nd edn. Wiley, New York
33. Wang J, Rivas G, Luo D, Cai XH, Valera FS, Dontha N (1996) DNA-modified electrode for the detection of aromatic amines. Anal Chem 68:4365–4369
34. Pan D, Zuo XL, Wan Y, Wang LH, Zhang J, Song SP, Fan CH (2007) Electrochemical interrogation of interactions between surface-confined DNA and methylene blue. Sensors 7:2671–2680
35. Yang W, Ozsoz M, Hibbert DB, Gooding JJ (2002) Evidence for the direct interaction between methylene blue and guanine bases using DNA-modified carbon paste electrodes. Electroanalysis 14: 1299–1302
36. Yan LJ, Wang XL, Li GJ, Lu YX, Gao HW, Sun W (2016) Electrochemical DNA sensor for Adh 1 gene sequence from corn endogenous with carbon microsphere modified electrode. Int J Electrochem Sci 11:9790–9799
37. Sun W, Lu YX, Wu YJ, Zhang YY, Wang P, Chen Y, Li GJ (2014) Electrochemical sensor for transgenic maize MON810 sequence with electrostatic adsorption DNA on

electrochemical reduced graphene modified electrode. Sensors Actuators B Chem 202:160–166
38. Qi XW, Gao HW, Zhang YY, Wang XZ, Chen Y, Sun W (2012) Electrochemical DNA biosensor with chitosan-Co_3O_4 nanorod-graphene composite for the sensitive detection of staphylococcus aureus nuc gene sequence. Bioelectrochemistry 88:42–47
39. Ensafi AA, Farfani NK, Amini M, Rezaei B (2017) Developing a sensitive DNA biosensor for the detection of flutamide using electrochemical method. J Iran Chem Soc 14:1325–1334
40. Mandli J, Mohammadi H, Amine A (2017) Electrochemical DNA sandwich biosensor based on enzyme amplified microRNA-21 detection and gold nanoparticles. Bioelectrochemistry 116:17–23
41. Fatemeh A, Seifati SM, Nasirizadeh N (2017) Development of a DNA biosensor for detection of phenylketonuria based on screen-printed gold electrode and hematoxylin. Anal Methods 9:966–973
42. Cai H, Cao X, Jiang Y, He P, Fang Y (2003) Carbon nanotube-enhanced electrochemical DNA biosensor for DNA hybridization detection. Anal Bioanal Chem 375:287–293
43. Peng HP, Hu Y, Liu P, Deng YN, Chen W, Liu AL, Chen YZ, Lin XH (2015) Label-free electrochemical DNA biosensor for rapid detection of mutidrug resistance gene based on au nanoparticles/toluidine blue–graphene oxide nanocomposites. Sensors Actuators B Chem 207:269–276
44. Wang L, Lin LQ, Xu XW, Weng SH, Lei Y, Liu AL, Chen YZ, Lin XH (2012) Electrochemical biosensor for detection of PML/RARα fusion gene based on eriochrome cyanine R film modified glassy carbon electrode. Electrochim Acta 69:56–59
45. Ren Y, Jiao K, Xu GY, Sun W, Gao HW (2005) An electrochemical DNA sensor based on electrodepositing aluminum ion films on stearic acid-modified carbon paste electrode and its application for the detection of specific sequences related to bar gene and CP4 Epsps gene. Electroanalysis 17:2182–2189
46. Jia F, Duan N, Wu SJ, Ma XY, Xia Y, Wang ZP, Wei XL (2014) Impedimetric aptasensor for Staphylococcus Aureus based on nanocomposite prepared from reduced graphene oxide and gold nanoparticles. Microchim Acta 181:967–974